Stationary Gaussian noises; noises in microwave and optical oscillators

François Bondu

Stationary Gaussian noises
Noises in microwave and optical oscillators

François Bondu

September 2024

Institut FOTON, UMR6082, CNRS / Université de Rennes, Rennes, France

Introduction : noisy measurements

In experimental sciences, time domain noises and signals are not easily analyzed simultaneously without a proper model. In this document we name "signal" a deterministic continuous time data, giving an information; a "noise" has a random nature; a "measurement" is the collected data where the signal is buried or covered with noise. Mathematically, a measured deterministic signal is almost always continuous with time variable t, and its Fourier transform also continuous; whereas the transform of a noise is not continuous nor derivable at any point on the frequency axis f. These mathematical struggles are properly handled with concepts such as power spectral density, signal-to-noise ratio, matched filtering. We present the not-well-known definition of a time domain noise by Cramér with a Stieltjes-Fourier integral; we recall the power spectral density estimator discovered by Thomson, not spread enough, except in the geophysics community. We will see that the signal-to-noise is not necessarily easy to appreciate on time domain measurements. This document will not address the noises specific to digitization. We will only consider linear time-invariant systems measuring a scalar real valued data.

This document aims at improving the knowledge of hopefully useful models for students dealing with experimental devices.

This document is strongly influenced by the professional practice of the scientific communities in which I participate: gravitational wave detectors, instrumentation with systems incorporating microwaves and lasers, noises in instruments, optoelectronics instrumentation design.

Keywords

Measurements; experimental physics; instrumentation; microwaves; continuous lasers; amplitude noise; phase noise; frequency noise; Friis formula; thermal noise; shot noise; amplified spontaneous emission (ASE).

1 Stationary Gaussian noise model

1.1 Continuous variables

Let's consider $n(t)$ a real valued noise with zero average. Following the initial works on Brownian noise of P. Lévy, A. Kolmogorov and N. Wiener, H. Cramér described a continuous noise with a Stieltjes-Fourier integral (eq. (11) in [1]), a linear superposition of infinitesimal sinusoidal waveforms with random amplitudes :

$$n(t) = \int_0^\infty \mathrm{d}n_{rms}(f)\sqrt{2}\cos(2\pi ft + \phi_n(f)) \tag{1}$$

when defined with positive frequencies values only; with negative frequencies we have the equivalent writing:

$$\boxed{n(t) = \int_{-\infty}^{\infty} \mathrm{d}n_c(f)\ \exp(i2\pi ft)} \tag{2}$$

where the complex valued amplitude is defined by :

$$\mathrm{d}n_c(f) = \frac{\sqrt{2}}{2}\,\mathrm{d}n_{rms}(f)\exp(i\phi_n(f)) \tag{3}$$

The Stieltjes-Fourier integral is not a Fourier transform. Technically the Stieltjes integral $\int f(x)\,\mathrm{d}g(x)$ exists if $\mathrm{d}g(x)$ is a finite increment function. The variables $\mathrm{d}n_c(f)$ have the properties :

- since $n(t)$ is a real valued function,

$$\mathrm{d}n_c^*(f) = \mathrm{d}n_c(-f) \tag{4}$$

  where x^* is the complex conjugate of x;

- the spectral components at two different frequencies are independent variables: $\langle \mathrm{d}n_c(f)\,\mathrm{dn_c}(f')\rangle = 0$ if $f \neq f'$ with $f, f' > 0$;

- The power spectral distribution power spectral density (PSD) $S_n(f)$ is defined by the variance:

$$\boxed{S_n(f)\,\mathrm{d}f = \left\langle |\mathrm{d}n_{rms}(f)|^{\,2}\right\rangle} = 2\left\langle |\mathrm{d}n_c(f)|^{\,2}\right\rangle \tag{5}$$

  where $\langle x\rangle$ is the statistical ensemble average of variable x.

- the spectral components may be decomposed into two real valued quadratures $\mathrm{d}n_{Ic}(f)$ and $\mathrm{d}n_{Qc}(f)$ with $\mathrm{d}n_c(f) = \mathrm{d}n_{Ic}(f) + i\,\mathrm{d}n_{Qc}(f)$; These quadratures are random variables with a Gaussian distribution, have a zero average and identical variances:

$$\left\langle |\mathrm{d}n_{Ic}(f)|^{\,2}\right\rangle = \left\langle |\mathrm{d}n_{Qc}(f)|^{\,2}\right\rangle = \frac{1}{4}S_n(f)\,df. \tag{6}$$

  Therefore the quantity $|\mathrm{d}n_{rms}(f)|$ follows a Rayleigh distribution.

Remarks:

- It is usual to index S with the variable whose PSD is measured. For example the PSD of a phase noise $\varphi(t)$ is written $S_\varphi(f)$.
- $\mathrm{d}n_c(f)$ is a random variable, discontinuous at all f; the PSD is deterministic, continuous and derivable, except at some points if pure sinusoidal components are considered.
- The noise $n(t)$ does not display, in the general case, a Gaussian distribution, except if it is a white noise. In a « Gaussian » noise, the quadratures $\mathrm{dn_{Ic}}(f)$ and $\mathrm{dn_{Qc}}(f)$ are the variables with a Gaussian distribution.
- If the physical measurement $n(t)$ has a unit u: $[n(t)] = \mathrm{u}$, then the unit of the PSD $[S_n(f)] = \mathrm{u}^2/\mathrm{Hz}$. Whatever the unit of u, the 1/Hz is a tag for a PSD and never simplified. Specifically, for a time domain frequency noise $\nu(t)$, measured in Hz, the PSD has the unit $[S_\nu] = \mathrm{Hz}^2/\mathrm{Hz}$.
- Some communities prefer to use standard deviation rather than variances. The "linear spectral density" is simply

$$\tilde{n}(f) = \sqrt{S_n(f).} \tag{7}$$

  If $[n(t)] = \mathrm{u}$, then $[\tilde{n}(f)] = \mathrm{u}/\sqrt{\mathrm{Hz}}$. There is a tradition of using power spectral densities in radiofrequency and microwave communities and linear spectral densities in instrument design.
- The PSD can be expressed in log scales, favored in the microwave community:

$$S_{n,dB} = 20\log_{10}\left(\tilde{n}(f)\right) = 10\log_{10}\left(S_n(f)\right)\ [\mathrm{dB\,u^2/Hz}] \tag{8}$$

- The equation 5 differs by a factor of 2 with the one used in the probability literature [1], $S_{th,n}(f) = \left\langle |\mathrm{d}n_c(f)|^2 \right\rangle$. Indeed, in probability theory, both negative and positive frequencies are considered, the PSD is "bilateral". In experimental sciences, one considers only positive frequencies: $S_n(f) = 2S_{th,n}(f)$: the PSD is "monolateral".
- The "power" in the expression "power spectral density" is not, in probability theory, a physical power in watts, but a variance. If $n(t)$ is a voltage measured across a resistor, the physical dissipated power dissipated at the frequency f in a bandwidth $\mathrm{d}f$ is:

$$P_f = \frac{S_n(f)\,\mathrm{d}f}{R} \tag{9}$$

  and $\tilde{n}(f)\sqrt{\mathrm{d}f}$ represents the root mean square (r.m.s.) value of the voltage at frequency f.

1.2 Digitized and sampled quantities

The kth sample of a digital series (or of a sampled noise with period T_s) writes [2]:

$$n[k] = \int_{-F_N}^{F_N} dZ(f)\ \exp(i2\pi f k T_s) \tag{10}$$

where the Nyquist frequency F_N is defined with $F_N = 1/(2T_s)$. The Cramér formula for a digitized noise is then:

$$S_n(f)\, df = 2\left\langle |dZ(f)|^2 \right\rangle \tag{11}$$

where $S_n(f)$ corresponds to the mono-lateral power spectral density.

1.3 White and colored noises

A "white noise" is a continuous random variable where $S_n(f) = S_0$ is constant with f.

A pink noise is such that $S_n(f) = \alpha/f$, with α a positive constant.

A "Brownian" noise is equivalent to a white noise filtered by an integrator. Its PSD is then $S_n(f) = \alpha/f^2$.

2 Estimators of PSD

The mathematical statisticians define the PSD with the ensemble average $\langle x \rangle$ of a very large number of identical systems. In the laboratory we rather most often have only one system, or at best a small numbers or "identical" systems. The noise is not measured on an infinite duration. Thus there is no way to "measure" the PSD, one has to use estimators as reliable as possible. The question of bias and estimator variance is of importance: the paper by Thomson in 1982 [3] discusses the good properties of estimators. The estimators in experimental sciences that I know of always consider only positive frequencies (monolateral spectral densities). Before going into the description of estimators the concept of filter equivalent noise bandwidth is going to be useful later on.

2.1 Filter equivalent noise bandwidth (ENB)

The ENB of a filter helps to understand the frequency resolution of PSD estimators.

Let's consider a white noise feeding a low-pass filter $H(f)$. The output is a noise with a finite power $< s^2{}_{out} >$. The equivalent noise bandwidth $\mathrm{ENB_{LP}}$ is the bandwidth of an equivalent filter with constant transmission $|H_{max}|$ in that band, and transmission is null outside this band, so that the same power $< s^2{}_{out} >$ is measured:

$$\mathrm{ENB_{LP}} = \int_0^\infty \mathrm{d}f \frac{|H(f)|^2}{|H_{max}(f)|^2}. \tag{12}$$

For a simple first order low pass filter with cut-off frequency f_0, of response time $\tau = 1/(2\pi f_0)$, the ENB is:

$$\mathrm{ENB_{LP}} = f_0 \frac{\pi}{2} = \frac{1}{4\tau}. \tag{13}$$

Note that the ENB is not the 3 dB bandwidth. If the filter $w(f)$ is used for convolution in the frequency domain, then the ENB is defined with:

$$\mathrm{ENB}_{\mathrm{window}} = \int_{-\infty}^{\infty} \mathrm{d}f \frac{|w(f)|^2}{|w_{max}(f)|^2}. \tag{14}$$

Such a filter analyses the frequencies at$f_0 - f$ and $f_0 + f$ for which the input noise spectral density is not zero: it is necessary to take into account the negative frequencies of that window.

2.2 Estimators with autocorrelation function

2.2.1 Einstein-Wiener-Khintchine theorem

A continuous real valued noise variable $n(t)$ is written, using equation 4 and equation 2:

$$n(t) = \int dn_c^*(-f)\ \exp(i2\pi ft)$$

and with a variable change $f \to -f$

$$n(t) = \int dn_c^*(f)\ \exp(-i2\pi ft).$$

The autocorrelation function is

$$C_n(\tau) = \langle n(t)n(t+\tau)\rangle = \left\langle \left(\int dn_c(f)\ \exp(i2\pi ft) \right) \left(\int dn_c^*(f')\ \exp(-i2\pi f'(t+\tau)) \right) \right\rangle$$

and becomes after distribution of terms

$$C_n(\tau) = \int \int \langle dn_c(f) dn_c^*(f')\rangle \exp(-i2\pi f'\tau)\, \delta(f - f')$$

and then

$$C_n(\tau) = \int df\, \frac{1}{2} S_n(f)\ \exp(-i2\pi f\tau).$$

We thus have the theorem [4, 5, 6] giving the monolateral power spectral density as a Fourier transform of the autocorrelation function:

$$\int C_n(t)\ \exp(-i2\pi ft)\, dt = \frac{1}{2} S_n(f). \tag{15}$$

H. Cramér notes [1] that this theorem has convergence issues for some functions where spectral densities are however well defined.

2.2.2 Use

A too fast analysis would like to estimate the autocorrelation of time domain data to produce PSD: use ergodicity, estimate the auto-correlation of a finite sample and take the Fourier transform of that function. This would be the source of multiple bias errors. The problem of "spectral leaks" (see below 5.2) will not be taken seriously. This is not to be used, except for a white noise (where it is useless).

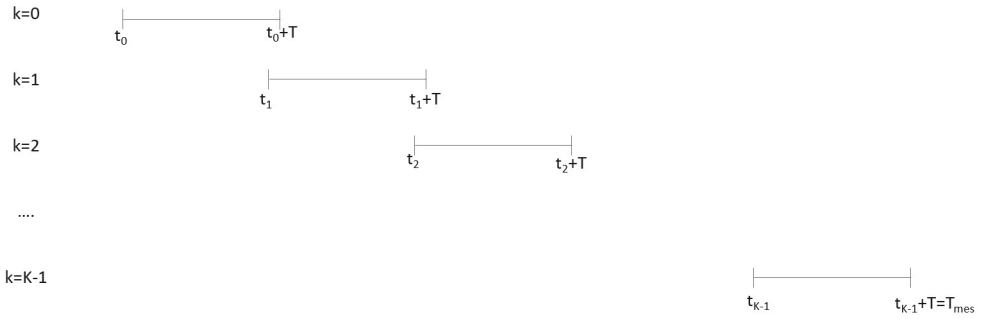

Figure 1: Slicing of the data for Welch method

2.3 Periodogram

This method is now completely obsolete. It consisted is computing a Fourier transform of the measurement $n(t)$ on a finite time interval $[0, T]$, and then smoothing its square modulus. The energy is not conserved and there are multiple biases. In that version, it is not used anymore; it is superseded by the Welch method.

2.4 Welch method

2.4.1 Definition

This method [7] is very popular, heavily used in commercial measurement instruments and in data processing software (Matlab, Python).

It consists in K measurements on slices of duration T of a stationary noise $n(t)$ starting from time t_0, cf. figure 1:

$$n_k(t) = n(t_0 + k\,T - \alpha_{\text{ovlp}} T) \tag{16}$$

where $0 \leq \alpha_{\text{ovlp}} < 1$ is a superposition factor (often equal to zero) and $k = 0, ..., K-1$ indexes the segment number. The data are sampled with a sampling period T_s, with M samples on each segment, so $T = MT_s$. On each segment data are numbered with $m = 0, ..., M-1$.
The power spectral density estimator is then:

$$\hat{S}_n(f) = \frac{2\,{T_s}^2}{T} \left[\frac{1}{K} \sum_k \left| FFT\left(n_k[m] \times w[m]\right) \right|^2 \right] \tag{17}$$

where $w[m]$ is an apodization window defined on the $[0, T]$ interval. For the noise power to be conserved, the window needs to conserve it for a white noise. As the variance of a white noise has to be conserved, the window normalization needs to be:

$$\frac{1}{T} \int_0^T w^2(t)\,\mathrm{d}t = 1 \tag{18}$$

and for a digitized window:

$$\sum_{m=0}^{M-1} w^2[m] = M. \tag{19}$$

One of the most popular window is the Hann window:

$$w_{\text{Hann}}[m] = \sqrt{\frac{2}{3}} \left[1 - \cos\left(\frac{2\pi m}{M}\right)\right]. \tag{20}$$

A factor K = 20 gives a good smoothing of the PSD estimator. The Hann window in Python scipy.signal.windows.hann() or numpy.hanning() is not correctly normalized for PSD estimation.

2.4.2 Frequency resolution in Welch's method

A window ENB is the actual frequency resolution of a PSD estimator. We aim at computing the ENB of a window in equation 14. We note $\bar{w}(t)$ the window average. Most windows have a maximal value in the frequency domain at $f = 0$, so that $w_{max}(f) = w(f = 0) = T\bar{w}(t)$, using the definition of the Fourier transform. The numerator of equation 14 is computed using Parseval theorem,

$$\int_{-\infty}^{\infty} \mathrm{d}f \, |w(f)|^2 = \int_{-\infty}^{\infty} \mathrm{d}t \, |w(t)|^2, \tag{21}$$

so that using a window normalization, the window ENB is:

$$\text{ENB}_{\text{window}} = \frac{1}{T \, |\bar{w}(t)|^2}. \tag{22}$$

Hence for the Hann window one has the frequency resolution:

$$\text{ENB}_{\text{Hann}}(f) = \frac{1,5}{T}. \tag{23}$$

For a digitized window the ENB calculation uses:

$$\text{ENB}_{\text{window}} = M \frac{\sum_m |w[n]|^2}{|\sum w[n]|^2}. \tag{24}$$

The frequency resolution is bigger than the frequency spacing $\Delta F = 1/(MT_s)$.

2.4.3 Use with sampled data

Python With sampled data, scipy.signal.welch() returns a frequency vector and a vector of PSD data.

The input parameters are:

- the vector $x(n\,T_s)$ of sampled data, with $n = 0, ..., N-1$ and $N = \text{len}(x)$,
- $f_s = 1/T_s$the sample frequency (default value $f_s = 1$ Hz),
- window='hann' default window,

- nperseg=None: default segment length is M =256 points. To get K=20 averages, one needs to define nperseg=len(x)/K.
- noverlap=None: segments do not overlap by default. If segments overlap, the statistical independence of data is not verified anymore, so that there is no real advantage to have $\alpha_{\text{ovlp}} \neq 0$.
- nft=None: FFT length, by default identical to the segment length (no zero padding).
- detrend='None': the non-default 'detrend'=linear gives better results if the data has non-zero slopes on segments, for example on a red-colored noise.
- return_onesided=True: returns the monolateral spectral density for real-valued data.
- scaling='density' : the PSD is calibrated in u^2/Hz coherent with a monolateral PSD; the scaling='spectrum' would return the Fourier transform in u^2, to make an easy read of the amplitude of lines if necessary.
- axis=-1 selects the axis for computing in case of multidimensional data.

Matlab The PSD command is named « pwelch ». The number of averages is controlled by the nfft parameter.

Use notes

- The maximal frequency of the spectrum is the Nyquist frequency $f_s = \frac{1}{2T_s}$. The interval between to successive frequencies ('bin') is $\Delta F = \frac{1}{MT_s} = \frac{1}{T}$. The frequency resolution of the spectrum is slighly bigger than ΔF, see later.
- If $\alpha_{\text{ovlp}} = 0$, each of the frequencies inside a bin frequency of width ΔF gets a different phase on different segments, so that they FFT's modulus are statistically independent.
- With $\alpha_{\text{ovlp}} = 0$, the interval between to successive frequencies is $\Delta F = \frac{1}{T} = \frac{K}{T_{mes}}$. Thus for a given measurement time, increasing the number of averages increases this interval.
- In case of a red-colored noise, the first two points of a spectrum (frequencies ΔF and $2\Delta F$) often have a strong bias, cf. 5.2, possibly because of the calibration (equation 14) becoming unaccurate. To avoid a wrong physical interpretation of these biased values, I would recommend to deliberately not display them.

2.4.4 Windows and spectral leaks

Historically, the first windows were thought as to smooth the data gently to zero on the segment sides, thus the name of "apodization". But the real problem is the one of spectral leaks. Indeed, as a noise data is sampled and multiplied with a window w_T, the data used for calculations is actually

$$n'[m] = n[m] \times w_T[m] \tag{25}$$

so that in the frequency space we have a convolution:

$$\mathrm{d}n'(f) = \mathrm{d}n(f) \star w_T(f). \tag{26}$$

Then the real spectrum is convoluted, as shown in [3]:

$$S_{n'}(f') = \int_0^\infty df\ |w(f - f')|^2\, S_n(f'). \tag{27}$$

Note that there is no way to avoid this effect: since a window has a finite duration, its spectrum can not be a Dirac function.The mixing of spectral components is not avoidable and biases the spectral components. The window w_T is designed to reduce this "leaking" effect. The evaluation of windows one has to compare their spectral performance [8]:

- Different windows have different ENB.
- The spectral leaks are reduced if the first sidelobe has a low relative amplitude (-32 dB for a Hann window), and if the following sidelobes have a steep slope ($1/f^3$ for a Hann window), efficient in the case of red-colored noise or in the presence of sinewaves in the noise data.
- The total leak is expressed with

$$\epsilon_{\mathrm{leak}} = 1 - \frac{\int_0^{\mathrm{ENB}/2} \mathrm{d}f\, |w(f)|^2}{\int_0^\infty \mathrm{d}f\, |w(f)|^2}; \tag{28}$$

  its value for a Hann window is ϵ_{leak} =17,9 %.
- The is a trade-off between frequency resolution and spectral leakage.

There is no "no window option". The rectangular window $w_T(t) = 1$ has an ENB= $1/T$, the first sidelobe is at -13 dB, and the sidelobe slope is $1/f$: the rectangular window is poor for PSD estimation for a colored noise or in the presence of sinewaves. There had been multiple researches for the "best" window, cf. for example [9]. However, the window really minimizing the spectral leaks is the Slepian window, as we will see in the next section.

2.5 Thomson method

The Thomson PSD estimator is also called "multitaper spectrum". To my knowledge, it is not widely used except by geophysicists. It does not seem to be implemented in commercial spectrum analyzers, although it would present advantages, for a given measurement time. The biases are better controlled. For identical average number, the frequency resolution and smallest frequency accessible are much better than with Welch method. An error bar of PSD is available. A PSD can be provided with a reliability estimate. The difficulty is with the computation of the window; however, there have been many recent works by the mathematicians to have fast and accurate Slepian windows available.

The Welch estimator slices the total measurement time $T_{mes} = KT_s$ into K segments of length M points, each segment providing a statistical independent

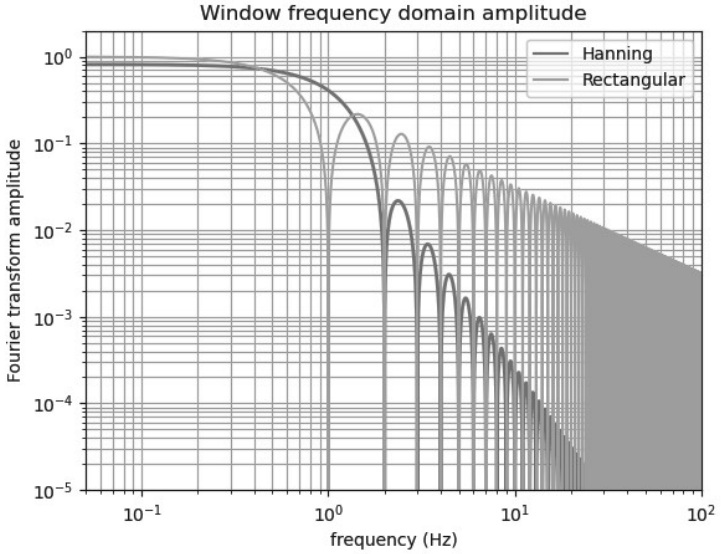

Figure 2: Spectral response of the rectangular and Hann windows

data for the PSD estimate; the total number of points is $N = KM$. The Thomson estimator uses orthogonal windows on a unique data segment, providing the statistical independency of the estimates. D. Thomson, to reduce spectral leakage, noted that the specification is to maximize the window energy in a low frequency band. The functions verifying this property are the "Slepian" function set, also called "prolate spheroidal wave functions" of order 0 [10, 11, 12]. The functions, defined on a finite segment, are orthogonal to each other. They are the eigenfunctions of the convolution with a cardinal sinus. The functions look like Hermite-Gauss function; they are actually a generalization of these functions on a finite duration interval.

The frequency resolution is a free parameter to be chosen. The factor "NW" is the factor that multiplies the frequency spacing $1/NT_s$ (for a Hann window, $NW = 1{,}5$). The number of averages will be roughly

$$K = \lfloor 2 \times NW \rfloor - 1$$

where $\lfloor x \rfloor$ is the integer part of the real x: the choice of NW impacts the average number. To have an equivalent of the Welch method, $NW = 10, 5$ will take into account 20 averages.

The Slepian function of order 0 ψ_0 is the one that maximized the energy of the interval $[-NW/NTs, NW/NTs]$. The concentration factor is noted λ_k; it is the eigenvalue of the correlation with a cardinal sinus; is it also the amount of energy in the targeted frequency band. The second function ψ_1 is the second function orthogonal to ψ_0 to maximize the function in the frequency interval, etc. The values λ_0, λ_1,... are very close to 1 for $k \leq K$, and very close to 0 for the following orders. The factor $(1 - \lambda_k)$ is the out-of-band energy leakage that will contribute to biases in the PSD estimate.

These functions are then ideal as windows. They are named as PSWF (Prolate

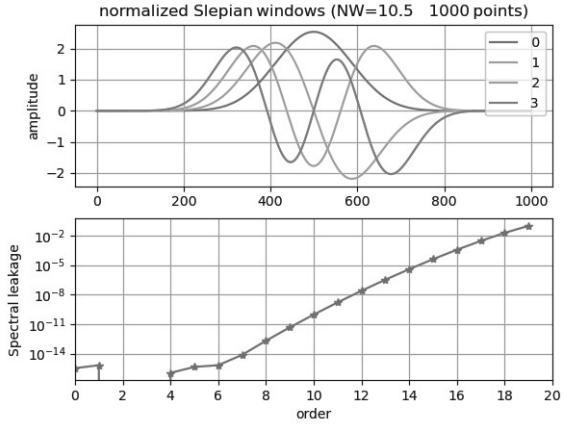

Figure 3: Slepian windows (prolate spheroidal wave functions of order 0) with indices 0 to 3. For the low order functions, the total spectral leak, much better than Hann functions, is actually limited by numerical resolution.

Spheroidal Wave Function) in the frequency domain. The Fourier transform of a Slepian function is a Slepian function with same order (but different scaling factors). The Fourier transforms are orthogonal on the maximum frequency concentration interval, and on the total frequency axis $]-\infty, +\infty[$. The discrete versions of the functions are called DPSS (Discrete Prolate Spheroidal Sequence).

The 1982 Thomson paper is very reach and worth a read. This method allows to give an error bar of PSD [13]. It gives a "stability" value, equivalent of a χ^2, ratio at each frequency bin of number of degrees of freedom to twice the number of used windows [3]. If this number is significantly below 1 on a frequency interval, the PSD is probably biased. There is no such reliability estimate for the Welch method. The Thomson paper might be confusing at times. G. Prieto has written a whole book describing all steps "multitaper spectrum estimation", 2008, availaible on demand, that describes the proper steps in the "adaptative weighing" flavor.

Python implementation

The Thomson method can be implemented with several flavors, based on different weighting of the windows for different indices [14]. The first method gives an equal weight to all windows; the second consists in weighting the windows with the eigenvalues; a third gives an adaptative weight to windows, in function of the context of other parts of the spectrum. This last one is the more robust for colored noises. The "multitaper" parameter implements this option since 2022 [15, 16]. It can also implement coherence functions (cf. section 5.2) and transfer functions. This package relies on the default DPSS implentation in Python.

The function scipy.signal.windows.dpss() uses the algorithm recommended in old "numerical recipes" versions [17], with the computation of eigenvalues and eigenvectors of a tridiagonal matrix. The function with option 'norm=2' should be multiplied by $\sqrt{M}$ to have a correct calibration as a window. The function

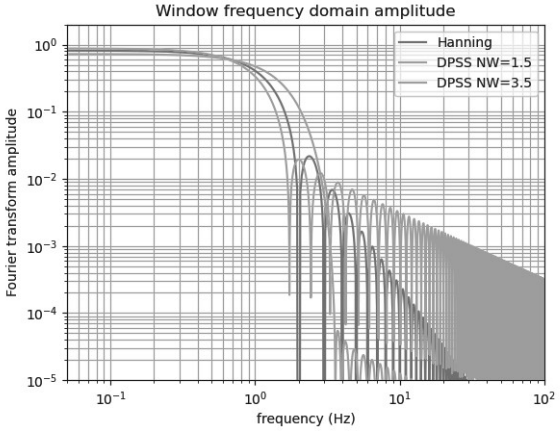

Figure 4: Slepian and Hann windows comparison

scipy.signal.windows.dpss() returns erroneous functions for $M > 92681$. It is not optimal for computing speed and accuracy, function orthogonality is not so good for high indices close to K, and eigenvalue accuracy not very good if the number of points is several thousands.

Recent researches in mathematics give a development of DPSS on a basis of Legendre polynomials to give a fast and accurate evaluation of PSWF [18, 19]. To our knowledge, no implementation of this in Python is available yet.

2.6 Comparison of Welch and Thomson estimators

For $K = 20$ averages and a Hann window, the frequency resolution with a Hann window on a total measurement time T is:

$$\mathrm{ENB}_{\mathrm{Welch,Hann}} = \frac{1,5K}{T} \tag{29}$$

whereas with the same number of averages, on the same measurement duration, the frequency resolution for $NW = K/2$ is

$$\mathrm{ENB}_{\mathrm{multitaper}} = \frac{NW}{T} \approx \frac{K}{2T}. \tag{30}$$

In these conditions, the frequency resolution is 3 times better for the Thomson estimator.

For identical frequency resolution $NW = 1,5\,K$, the Thomson estimator has better biases and reduced variance compared to the Welch estimator, and gives access to lower spectral frequencies. The Thomson estimator should take precedence other the Welch one, now that calculation difficulties are overcome.

Even when the NW parameter is small, the Slepian window is much better than the Hann one, cf. figure 4. The Hann window has a leak value of 17,9 %; with similar frequency resolution on a segment, NW=1.5, the order 0 Slepian window has a leak of 0.11%; With a slightly bigger frequency resolution, NW=3.5, the spectral leak is $6{,}3.10^{-9}$. Within the Welch method, the Slepian window should be preferred, when this window is available.

3 Noise in linear time-invariant systems

3.1 Independent noise sources

Given $n_1(t)$ and $n_2(t)$ two stationary noises, each described by a Fourier-Stieltjes integral, the sum of the two noises writes :

$$n(t) = n_1(t) + n_2(t) = \int (\mathrm{d}n_1(f) + \mathrm{d}n_2(f)) \exp(i2\pi ft). \tag{31}$$

If $\mathrm{d}n_1(f)$ and $\mathrm{d}n_2(f)$ are statistically independent variables it comes immediately that

$$S_n(f) = S_{n_1}(f) + S_{n_2}(f). \tag{32}$$

The two variances add up, hence the power spectral densities add up.

3.2 Noise through a system element

Given h a linear, time-invariant (LTI) system, for two input signals $x(t)$ and $y(t)$ and two real valued factors α and β, by definition,

$$h\left(\alpha x(t) + \beta y(t)\right) = \alpha h\left(x(t)\right) + \beta h\left(y(t)\right) \tag{33}$$

(linearity) and

$$\text{if } x(t) \text{ gives an output } x_{out}(t), \text{then } x(t+\tau) \text{ gives and output } x_{out}(t+\tau) \tag{34}$$

(time-invariance). The eigenvalues of such systems are the functions $\exp(i2\pi ft)$:

$$h\left(\exp(i2\pi ft)\right) = H(f) \exp(i2\pi ft) \tag{35}$$

where $H(f)$ is the Fourier transform of the impulse response $h(t)$. Then for a noise described by a Fourier-Stieltjes integral $n_{in}(t)$, using equation 33 one gets

$$H(n(t)) = \int (\mathrm{d}n_{in}(f) H(f)) \exp(i2\pi ft). \tag{36}$$

It is immediately apparent that the output power spectral density of system H has power spectral density

$$\boxed{S_{n,out}(f) = S_{n,in}(f) \times |H(f)|^2}. \tag{37}$$

$$\tilde{n}_{out}(f) = \tilde{n}_{in}(f) \times |H(f)|\,. \tag{38}$$

Lets take the example of an integrator system $H(f) = f_0/(if)$. A white noise at the input gives a Brownian noise at output ; the spectral noise density at the output has a shape α/f^2, where α is a positive constant.

Using equation 37 we demonstrate the formula for $\mathrm{ENB_{LP}}$ for a low-pass filter (equation 12). With a frequency independent (white noise) S_{in} at the filter input of $H(f)$, the output variance is

$$\left\langle {s^2}_{out}(t) \right\rangle = \int_0^\infty \mathrm{d}f\, S_{in} \times |H(f)|^2$$

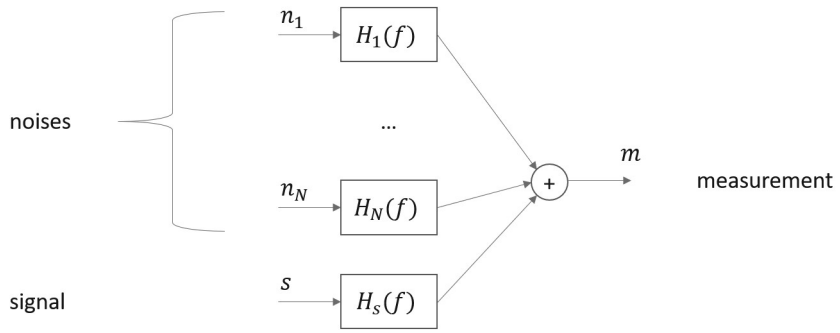

Figure 5: Instrumentation with several noise sources and a signal input

and the variance of a filter with constant transmission $|H_{max}|$ on a frequency bandwidth $\mathrm{ENB_{LP}}$ is

$$\left\langle {s^2}_{out}(t) \right\rangle = |H_{max}(f)|^2 \, \mathrm{ENB_{LP}}.$$

The definition of $\mathrm{ENB_{LP}}$ follows.

3.3 Instrument noise budget

Let's give an instrument subject to n_i independent parasitic noise sources, each with a transfer function $H_i(f)$ between the source and the instrument measurement channel, and a signal source with its transfer function, cf. figure 5.

Given the superposition principle seen above, the output noise will have a power spectral density:

$$S_{out}(f) = \sum S_{n_i}(f) \; |H_i(f)|^2. \tag{39}$$

The signal has a transfer function $H_s(f)$ with the measurement channel, also named "instrument sensitivity". Numerically it is possible to refer the noises as referred to the signal input, in signal unit:

$$S_{n,in}(f) = \frac{1}{|H_s(f)|^2} \sum S_{n_i}(f) \; |H_i(f)|^2. \tag{40}$$

The whole instrument is a sensor with noises sources referred to the input as in figure 7.

In the jargon of some scientific communities this input-referred noise is called "instrument sensitivity" (gravitational wave detection for example). Following the international vocabulary of metrology [20] it may be better named "detection limit spectral density". This curve is very useful, for a known expected signal, to understand where the instrument performance has to be improved, cf. figure 6.

3.4 Sensors

3.4.1 dynamic range

The maximal value of a sensor is a voltage; its noise linear spectral density is in $\mathrm{V}/\sqrt{\mathrm{Hz}}$. The dynamic range is the ratio of the maximal value to the noise

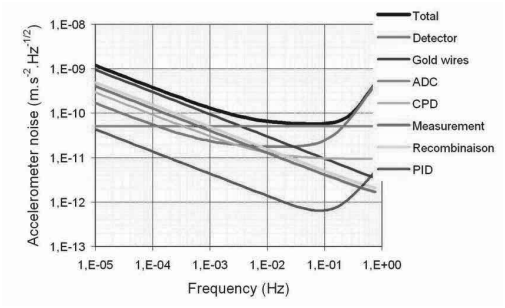

(a) Noise budget (linear spectral density) for the noise sources of the MicroSTAR accelerometer ([21])

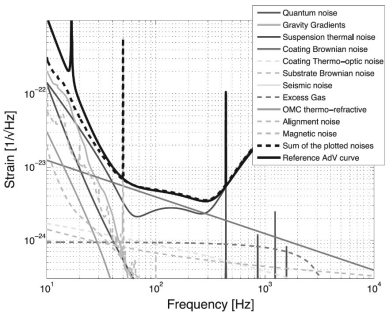

(b) Planned noise budget for the gravitational wave detector Virgo in 2021 ([22])

Figure 6: Examples of instrument noise budget PSD

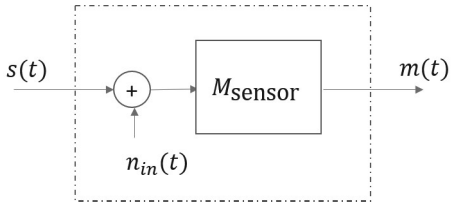

Figure 7: input referred noise of a sensor

linear spectral density, and is frequency dependent. In commercial datasheets the "dynamic range" is often unitless, using non-specified additional parameters such as supposed integration time of a filter of unknown shape. The commercial practice of private companies would make the engineer life easier by giving both transfer function and input-referred noise spectral density instead.

3.4.2 Input noises in electrical and optical sensors

Sensors are converting the physical quantity they measure into a voltage via a transfer function $M(f)$. The physical quantity is measured together with its intrinsic noise. For example, an electrical voltage is measured together with thermal noise; an antenna senses an electric field, together with its shot noise; an optical beam is measured together with its shot noise. The sensor, often active, also has intrinsic sources of noises, named "read-out noise". All additional noises present at the output are referred to the sensor input.

A voltage sensor will have a readout noise PSD S_V in V^2/Hz. With a known impedance R, for example in a 50 Ω system in microwaves, it can be also expressed as a power S_V/R in W/Hz. A photodiode senses an optical power; the readout noise is thus in W^2/Hz.

3.5 Noise in servo loops

A servo loop may be represented by one of the schematics in figure 8 where $M(f)$ is a sensor transfer function, $A(f)$ actuator transfer function, and $C(f)$ the one for the electronic correction (PID for example).

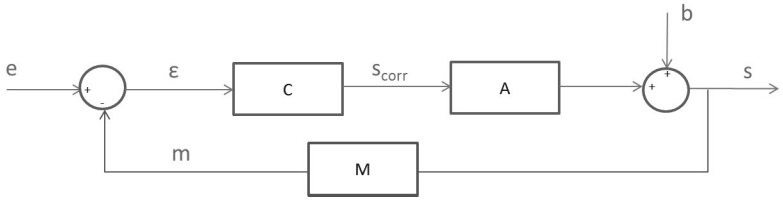

(a) Standard feedback loop

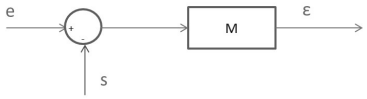

(b) Sensor in metrology

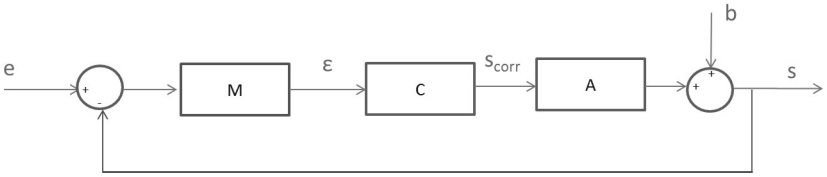

(c) Servo loop in metrology

Figure 8: Several simple feedback loops

In a standard feedback loop as in fig. 8a, a sensor delivers a voltage $m(t)$ that is compared to a reference level or command $e(t)$ to give an error $\epsilon(t)$. The correction circuitry filters the electrical signal to provide a correction signal $s_{\rm corr}(t)$ to the actuator. The feedback loop may be used to attenuate the effect of a perturbation signal $b(t)$ to give a more accurate output $s(t)$. In fig. 8c a loop in a metrology experiment, the sensor (fig. 8b) compares two physical quantities, a reference level $e(t)$, ideally constant, and the system output $s(t)$. The open loop transfer function is in both cases in the frequency domain:

$$G_{bo} = M(f)\, C(f)\, A(f) \tag{41}$$

In the case of a metrology loop, if the inputs are deterministic signals, then the equations between of the Fourier transforms of the input signals (reference and noise inputs) and the outputs (output physical quantity, measurable error and correction signals) are:

$$s_{\rm out}(f) = \frac{G_{bo}}{1+G_{bo}} s_{\rm ref}(f) + \frac{1}{1+G_{bo}} b(f) \tag{42}$$

$$\varepsilon(f) = \frac{M}{1+G_{bo}} s_{\rm ref}(f) - \frac{M}{1+G_{bo}} b(f) \tag{43}$$

$$s_{\rm corr}(f) = \frac{1}{A}\frac{G_{bo}}{1+G_{bo}} s_{\rm ref}(f) - \frac{1}{A}\frac{G_{bo}}{1+G_{bo}} b(f) \tag{44}$$

The frequency dependence of transfer functions M, C, A, G_{bo} is omitted to have lighter notations. For the Fourier frequencies such that $|G_{bo}| \gg 1$, the correction signal is a sensor of s_{ref} and b with transfer function $1/A$.

If the perturbation noise $b(t)$ and reference signal $s_{\text{ref}}(t)$ are time domain independent random variables described with Fourier-Stieltjes integrals, then using equation 39 one can give the power spectral density of of physical quantities and measurable voltages:

$$S_{\text{out}}(f) = \left|\frac{G_{bo}}{1+G_{bo}}\right|^2 S_{\text{ref}}(f) + \left|\frac{1}{1+G_{bo}}\right|^2 S_b(f) \tag{45}$$

$$S_{\varepsilon}(f) = \left|\frac{M}{1+G_{bo}}\right|^2 S_{\text{ref}}(f) + \left|\frac{M}{1+G_{bo}}\right|^2 S_b(f) \tag{46}$$

$$S_{\text{corr}}(f) = \left|\frac{1}{A}\frac{G_{bo}}{1+G_{bo}}\right|^2 S_{\text{ref}}(f) + \left|\frac{1}{A}\frac{G_{bo}}{1+G_{bo}}\right|^2 S_b(f) \tag{47}$$

$S_{\varepsilon}(f)$ measures the ultimate performance of the feedback loop; an out-of-loop measurement is often necessary in metrology to ensure the real performance. In the context of metrology experiments, the feedback loop is realized because the reference has a much smaller PSD than the perturbation, $S_b(f) \gg S_{\text{ref}}(f)$. Then the correction signal in eq. 47 shows that the correction signal is a sensor of $S_b(f)$ with calibration factor $1/|A(f)|^2$. To really benefit of the full advantage of the reference, one has to ensure that the loop gain $|G_{bo}|$ is large enough such that $S_{\text{ref}}(f) \gg S_p(f)/|G_{bo}|^2$; then the physical output signal s_{out} follows the reference $S_{\text{out}}(f) \approx S_{\text{ref}}(f)$.

3.6 Spectrum analyzers

3.6.1 Electrical spectrum analyzers (ESA)

The «RBW» (Resolution Bandwidth) of an electrical spectrum analyzer is the frequency spacing; it is not the noise equivalent bandwidth. The "old" instruments (cathodic screen, analog data processing) display the power in dBm in a frequency band RBW. To convert into spectral density, the data has to be calibrated with

$$S_V = \frac{10^{-3}\,10^{P_{dBm}/10}}{\text{ENB}}\ [\text{W/Hz}]. \tag{48}$$

The ration between RBW and ENB is instrument-dependent [23]! In "modern" instruments (color screen, digital data analysis, "FFT mode",...) the ratio between RBW and ENB is close to 1 (for a Gaussian filter the ratio is 1.056), and taken into account for a display of calibrated data in $\text{V}/\sqrt{\text{Hz}}$ [24]. When measuring phase noise, the instrument manual makes it clear if the display is monolateral spectral density S_{φ}in $\text{dB rad}^2/\text{Hz}$ or bilateral spectral density $L_{\varphi,dB}(f) = S_{\varphi}(f) - 3\text{dB}$ in dBc/Hz. For instance the Rohde&Schwartz FSW estimates $L_{\varphi,dB}(f)$.

3.6.2 Optical spectrum analyzers (OSA)

The optical spectrum analyzers rarely precise the filter profile. The user's manual for Yokogawa AQ6380 makes it clear that the resolution bandwidth is defined at -3 dB, it is not the ENB. The filter shape is unknown. The user is left with measuring the OSA filter and compute its ENB, or approximate ENB to RBW.

3.7 Phase and frequency noises

The "system" can be also a variable integration, for example between frequency and phase. An oscillator output with phase noise is modeled with

$$s(t) = s_0 \sin\left(2\pi\nu_0 t + \varphi(t)\right) \tag{49}$$

where $\varphi(t)$ is a noise function. The instantaneous phase of this oscillator is

$$\Phi(t) = 2\pi\nu_0 t + \varphi(t) \tag{50}$$

and the instantaneous frequency can be defined with [20]

$$\nu_{\text{inst}}(t) = \frac{1}{2\pi}\frac{\mathrm{d}\Phi}{\mathrm{d}t} = \nu_0 + \frac{1}{2\pi}\frac{\mathrm{d}\varphi}{\mathrm{d}t}. \tag{51}$$

There is therefore the transfer function if between phase noise and frequency variations, and the relationship between PSD for phase and frequency noises:

$$S_{\delta\nu}(f) = f^2 S_\varphi(f). \tag{52}$$

When considering the phase noise of microwave oscillators, historical reasons (availability of electrical spectrum analyzer, where the carrier is displayed without demodulation) have led to consider separately the noise sidebands at $+f$ et $-f$ relative to the carrier ν_0 frequency. In that case $L(f) = S(f)\,/\,2$ [20]. In that context, $S_\varphi(f)$ is a monolateral PSD (only positive frequencies) whereas $L(f)$ is a bilateral PSD. $L(f)$ is measured a single side band (SSB) relative to the carrier. It is common in microwave community to take log scales. The unit of $S_{\varphi,dB}(f) = 10\log_{10}(S_\varphi)$ is then «dB rad²/Hz» in log scale, whereas $L_{dB}(f) = S_{\varphi,dB} - 3$ dB is written « dBc/Hz », meaning that it shows the power of one of the sidebands relative to the carrier.

3.8 Coherence

3.8.1 Definition

It is hazardous to draw conclusions from the similarity of time data , as shown by several web sites on "spurious correlations". In the frequency domain, it is possible to define if random data have a common phase relationship on a frequency interval of finite length. It is then possible to draw a physical interpretation for causality or common source. It can be very useful on instrumentation science to debunk parasitic noise sources. If the coherence is close to 1, a transfer function can be estimated. The coherence between to noises n_x and n_y is defined in the frequency domain with:

$$C_{xy} = \frac{\left|\left\langle \mathrm{d}n_x(f)\,\mathrm{d}n_y^*(f)\right\rangle\right|^2}{\left\langle\left|\mathrm{d}n_x(f)\right|^2\right\rangle\left\langle\left|\mathrm{d}n_y(f)\right|^2\right\rangle}. \tag{53}$$

The statistical average on the numerator will tend to zero for uncorrelated data, and $C_{x,y}$ tends to 1 if noises are proportional to each other with a constant phase delay. The coherence function is implemented on several vector signal analyzers (VNA), for example on the SR780 from Stanford Research Systems.

3.8.2 Crosscorrelations for phase noise measurements

The measurement of the phase noise φ_{DUT} of a high performance oscillator can be compared to two different local oscillators. The coherence of $\varphi_{DUT}(t) - \varphi_{OL1}(t)$ and $\varphi_{DUT}(t) - \varphi_{OL2}(t)$, if not zero, makes it possible to measure phase noise below the phase noise floor of each of the local oscillators.

4 Signal to noise ratio

We want here to know in a measurement $m(t) = s(t) + n(t)$ with how much certainty we have a signal $s(t)$ embeded in a noise $n(t)$. Within an instrumentation, the presence of noise in the same bandwidth as the signal is unavoidable, either being technical noises or fundamental noises (quantum noise, thermal noise). All measurements are real-valued here.

4.1 Finite energy signals

4.1.1 Definition

The signal-to-noise ratio (SNR) is defined with:

$$\boxed{\frac{S}{N} = \int_0^\infty \frac{2\left|s(f)\right|^2}{S_n(f)}\,\mathrm{d}f.} \tag{54}$$

The signal-to-noise "ratio" is the sum of the ratios of signal power to noise power per infinitesimal frequency bands. It has no physical units. Note that the signal to noise is sum of ratios, not a direct ratio in the general case. This formula holds for monolateral noise power spectral density. The factor of 2 stands for the negative frequencies of the Fourier transform of $s(t)$.

In the case the time domain noise is white noise, then its spectral density is frequency independent. Then the noise PSD can be factorized in the front of the integral. Then, using Parseval's theorem,

$$\frac{S}{N} = \frac{\int_{-\infty}^{\infty} \left|s(t)\right|^2\,\mathrm{d}t}{S_n} \tag{55}$$

In that specific case, the signal-to-noise is the ratio of the energy of the signal to the noise PSD.

4.1.2 Signal to noise ratio and filtering

We want to know how filtering a signal and noise data stream improves or degrades the signal to noise. The filter has a transfer function $H(f)$. The noise PSD becomes

$$S_n(f)\left|H(f)\right|^2,$$

whereas the signal PSD becomes

$$2\left|s(f)H(f)\right|^2\mathrm{d}f.$$

Then in the signal-to-noise ratio, as defined in equation 54, $\left|H(f)\right|^2$ simplifies simultaneously on numerator and denominator. The signal to noise ratio is thus

unchanged. Actually, with an analog filtering, a little noise will be added by the filter, slightly degrading the signal to noise ratio.

In case of red-colored noise, the signal-to-noise can be quite good, even if not visible by the eye. The SNR is not "what you see is what you get". Time domain data can be misleading to have an eye appreciation. At the first detection of gravitational waves on LIGO detectors in September 2015, the "signal" was visible by the eye on the interferometer dark fringe, an error signal of a servo loop. However, when "calibrating" the data with the instrument transfer function (cf. equation 40), the noise is red-colored and the signal disappears in the noise. The publication [25] showed the calibrated time domain data with a high-pass filter so that one may appreciate by the eye the signal shape. Without the high-pass filtering, the signal would have been invisible. However, the SNR as defined by equation 54 remained the same. There is no denial of the pedagogical effect of a visible time domain data; but the scientific conviction lies in the SNR and the associated false alarm rate.

4.1.3 Matched filtering

In a real data stream the measurement $m(t) = s(t - t_0) + n(t)$ does not allow an immediate calculation of signal to noise, and the arrival date of the data t_0 can be unknown. If the prototype signal is $s_0(t)$ is known, then a matched filter can answer the questions: is the signal present? when? what size? The signal theory shows that the optimal linear filter has a frequency response [26]:

$$h_{\text{match}}(f) = \frac{s_0^*(f)}{S_n(f)}. \tag{56}$$

If the noise is white, S_n is frequency independent, and the filter is, up to a scale factor, the signal expected reversed in time. In the presence of noise alone at the input, the output of a matched filter is a white noise.

The filter output will be monitored with a trigger level (for example 3 times the signal prototype integrated square modulus); the output is maximal at the signal arrival time; the output amplitude gives the signal amplitude with respect to the prototype one, and is roughly also the signal to noise ratio.

A matched filter can be installed at the instrument output, for example $m(t)$ in fig. 5; the noise in that case is the output noise $S_n(f)$. The measurement can be calibrated by a convolution with a filter h_{cal}(t)whose transfer function is $H_{\text{cal}}(f) = 1/H_s(f)$; the noise in the matched filter formula is in that case the noise referred to the input $S_{n,in}(f)$. The signal to noise ratio is identical in both cases. The signal is easier to see "by the eye" in the case where the noise is white.

4.2 Finite power signals

4.2.1 Context

Carriers modulated in phase and/or in amplitude go through different elements of a system: photodiode or antenna; propagation lines; amplifiers; filters; etc. The modulated signal lies in a bandwidth $[F_0 - B/2, F_0 + B/2]$. In these contexts one assumes usually that the noise PSD in frequency independent.

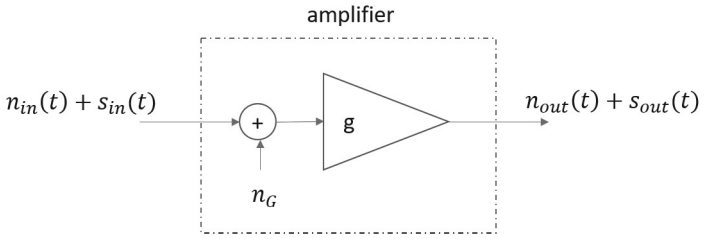

Figure 9: A system with noise referred to the input

4.2.2 Definition

The signal to noise ration is the signal power to the noise PSD times the signal bandwidth:

$$\boxed{\mathrm{SNR} = \frac{P_{\mathrm{signal}}}{P_{\mathrm{noise}}} = \frac{\langle s^2(t) \rangle}{S_n \times B}.} \tag{57}$$

The Carrier-to-Noise ratio (CNR) is defined by:

$$\mathrm{CNR} = \frac{P_{\mathrm{signal}}}{PSD_{\mathrm{noise}}} = \frac{\langle s^2(t) \rangle}{S_n}. \tag{58}$$

The physical unit for CNR is Hz (or dB.Hz in logarithmic scale).

4.2.3 Noise factor of a system element

A system element, for example an amplifier, may have multiple noise inputs. The whole behavior, in the operating conditions (input signal amplitude, system gain, saturation level, etc.) is modeled with an equivalent noise referred to the input, as in figure 9. In these situations both the gain and noise noise PSD are assumed to be frequency independent in the working bandwidth.

The noise factor describes the degradation of signal to noise while the input noise PSD $n_{in}(t)$ is equal to a pre-defined noise floor $S_{in}(f) = S_{in,\mathrm{floor}}$ [27] :

$$F = \frac{\mathrm{SNR}_{in,\mathrm{floor}}}{\mathrm{SNR}_{out}} \tag{59}$$

The signal to noise ratio at the input is, using equation 57:

$$\mathrm{SNR}_{in,\mathrm{floor}} = \frac{\langle {s_{in}}^2(t) \rangle}{S_{in,\mathrm{floor}} \times B} \tag{60}$$

and at the output, with $G = g^2$ being the power gain of the amplifier, and S_{nG} the PSD of the amplifier noise referred to the input:

$$\mathrm{SNR}_{out} = \frac{\langle G\, {s_{in}}^2(t) \rangle}{G\,(S_{n_G} + S_{in,\mathrm{floor}}) \times B}. \tag{61}$$

The noise factor can also be expressed as:

$$\boxed{F = 1 + \frac{S_{n_G}}{S_{in,\mathrm{floor}}}.} \tag{62}$$

The quantity $F-1$ is the ratio of input referred noise PSD to the floor PSD. For an electrical system, as the noise is proportional to temperature, the noise figure is

$$F_{\text{comp}} = 1 + \frac{T_{\text{eff}}}{290\ \text{K}} \tag{63}$$

where T_{eff} is the effective noise temperature. The temperature describes the noise in components in millimeter and submillimeter elements.

When expressed in dB, the noise factor becomes the noise figure:

$$F_{dB} = 10\log_{10}(F). \tag{64}$$

The PSD in equation 62 being positive whatever the component, even when the component is a simple lossy propagation ($G < 1$), it is obvious that

$$F \geq 1. \tag{65}$$

$F = 1$ would apply for a system not adding any noise at all. A filter with $F = 2$ ($F_{dB} = 3$ dB) degrades the signal to noise with a factor 2, if the input signal is limited by its noise floor.

It is possible to find electrical amplifiers with $F<2$. For example the amplifier ZKL-33ULN-S+ at Mini-Circuits is a 400 MHz - 3 GHz amplifier with noise figure of only 0,36 dB at 900 MHz. In the optical domain, the amplifiers operate on the power (photons) instead on electromagnetic field; the noise figure is always above 3 dB, for example the LNA-320 at Alnair. The development of amplifiers "sensitive to the phase" under way will eventually have noise figures smaller than 3 dB.

Note that an amplifier with a low noise factor is only needed if the input entry is such that its noise PSD is close to the noise floor. Assume an input with a noise PSD k times above the noise floor. Then the calculation of the signal to noise degradation leads to:

$$\frac{\text{SNR}_{in}}{\text{SNR}_{out}} = 1 + \frac{S_{nG}}{S_n} \tag{66}$$

$$= 1 + \frac{S_{nG}}{kS_{n,\text{floor}}} \tag{67}$$

$$= 1 + \frac{F-1}{k}. \tag{68}$$

For example, for an electrical system, if $k = 10$ and the amplifier used has a noise factor $F = 2$, the signal to noise degrades by a factor the very moderate value of 1.1.

4.2.4 Friis'Formula - cascaded elements

Assume now a system with various elements, for example an electrical system with antenna, amplifier, propagation cable, etc. It can be modeled as a chain of elements as in figure 10.

The calculation of the noise PSD at the output leads to:

$$S_{n,out} = (S_{n,in} + S_{nG1}) \times G_1 ... G_N + S_{nG2} \times (G_2 ... G_N) + ... + S_{nGN} \times G_N \tag{69}$$

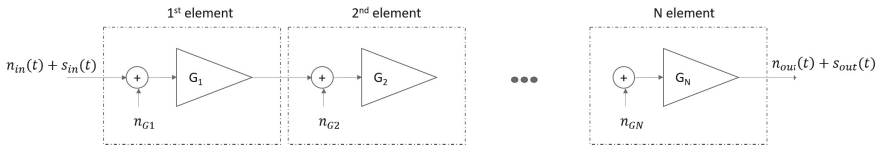

Figure 10: System of cascades elements

so that the noise of the whole system referred to the input is:

$$S_{syst,in} = \frac{S_{n,out}}{G_1 \times ... \times G_N} \tag{70}$$

$$= S_{n,in} + S_{nG1} + \frac{S_{nG2}}{G_1} + ... + \frac{S_{nGN}}{G_1 ... G_{N-1}}. \tag{71}$$

Replacing with the formula 62 for noise factor:

$$S_{nGi} = (F_i - 1) S_{n,\text{floor}} \tag{72}$$

one gets the noise factor for the whole system [27]:

$$\boxed{F_{sys} = F_1 + \frac{F_2 - 1}{G_1} + ... + \frac{F_N - 1}{G_1 ... G_{N-1}}.} \tag{73}$$

This formula shows that in a cascaded system, the noise factor of the first stage, usually a front-end amplifier, is the most important one. If the first element is a lossy propagation line, then the noise factor of the second element, an amplifier, is the important one.

4.2.5 Reference floor noise in electrical systems

In a microwave system, the carrier wavelength is usually smaller that the propagation lengths between the system elements. In that case the input and output impedances of each elements are identical and set to 50 Ω to insure maximum power transmission. A resistor R is modeled by a noiseless resistor in series with a voltage source of random noise of PSD

$$S_{V,R} = 4 k_B T_a R \ [\text{V}^2/\text{Hz}] \tag{74}$$

where k_B is the Boltzmann constant, T_a the absolute temperature in Kelvins (room temperature assumed to be 290 K), R_{50}=50 Ω. The voltage PSD is then 0,91 nV/$\sqrt{\text{Hz}}$. This value is the order of magnitude of noises referred to the input in very good operational amplifiers, for ex. LT1028 with 1,0 nV/$\sqrt{\text{Hz}}$. The electrical power (physical power) PSD is then

$$S_p = \frac{S_V}{R} = 4 k_B T_a \ [\text{W/Hz}]. \tag{75}$$

The reference floor noise is defined by the following ideal setup: the input of an instrument, assumed to be an ideal 50 Ω resistor, is connected with a source with a noiseless 50 Ω output impedance. The noise voltage generated by the

instrument input noisy impedance is divided on two resistors in series, so the reference noise floor voltage at the input is

$$S_{V,\text{floor}} = kT_a R_{50}\ [\text{V}^2/\text{Hz}]. \tag{76}$$

and the corresponding power noise on the input resistor

$$S_{P,\text{floor}} = kT_a\ [\text{V}^2/\text{Hz}]. \tag{77}$$

In dBm this amounts to -174 dBm/Hz, the minimum noise level in any 50 Ω system.

4.2.6 Reference floor noise in laser optics

The signal is carried on a field mode, an the electromagnetic field with a finite transverse section. We define here an optical mode signal as a real valued quantity $\psi(t)$ such that ψ^2 is the instantaneous power (in watts). With that signal, the reference floor is:

$$S_{\psi,\text{floor}} = 2h_P\nu_0\ [\text{V}^2/\text{Hz}] \tag{78}$$

where h_P is the Planck constant, and ν_0 the optical frequency of the carrier.

4.2.7 Phase and amplitude of oscillators in noise background

A measurement of an ideal pure sine signal in a white background noise will display amplitude and phase noise. In the frequency domain, the noise sidebands with frequencies smaller than the carrier and higher than the carrier are uncorrelated. This creates simultaneous phase and amplitude noise. Let's model a sinewawe with noise with the equation:

$$m(t) = m_0\sqrt{2}\cos(2\pi\nu_0 t) + n(t) \tag{79}$$

where m_0 is the root mean square value and $n(t)$ a real valued stationary noise with frequency independent PSD S_n. The power of the signal, either electrical or optical, is $P_0 = {m_0}^2$. The noise can be a reference noise floor or a technical noise. A technical noise for electrical carriers can be a readout voltage, the noise from an amplifier with a noise factor bigger than 1, etc. A technical noise for optical carriers can be the amplified spontaneous emission level of an amplifier, etc. The measurement can be rewritten:

$$m(t) = m_0\frac{\sqrt{2}}{2}\left(\mathrm{e}^{i2\pi\nu_0 t} + \mathrm{e}^{-i2\pi\nu_0 t}\right) + \int \frac{\sqrt{2}}{2}\left(dn_I(f+\nu_0) + i dn_Q(f+\nu_0)\right)\mathrm{e}^{i2\pi(\nu_0+f)t} \tag{80}$$

where $S_n = 4\left\langle |\mathrm{d}n_I(f)|^2 \right\rangle = 4\left\langle |\mathrm{d}n_Q(f)|^2 \right\rangle$, cf. equation 6. The corresponding analytical signal can be written:

$$m_a = m_0\mathrm{e}^{i2\pi\nu_0 t}\left(1 + \frac{1}{m_0}\int_{f=-\nu_0}^{f=+\nu_0}\left(dn_I(f) + i dn_Q(f)\right)\mathrm{e}^{i2\pi f t}\right). \tag{81}$$

Note that the limitation on the integral bounds has no practical limitation as the signal bandwidth B is much smaller than the carrier frequency ν_0.

The relative amplitude noise is then:

$$n_a(t) = \frac{1}{m_0} \int_{f=-\nu_0}^{f=+\nu_0} dn_I(f) \mathrm{e}^{i2\pi ft} \tag{82}$$

and the phase noise is:

$$n_\varphi(t) = \frac{1}{m_0} \int_{f=-\nu_0}^{f=+\nu_0} dn_Q(f) \mathrm{e}^{i2\pi ft}. \tag{83}$$

The usage is to consider the "relative intensity noise", rather than the relative amplitude noise, i.e. defined as the noise of $|m_a(t)|^2 \approx P_0(1 + 2n_a(t))$. Thus

$$S_{RIN} = \frac{S_n}{P_0} \tag{84}$$

and the phase noise is:

$$S_\varphi = \frac{S_n}{4P_0}. \tag{85}$$

For a shot-noise limited monochromatic laser beam

$$S_{RIN,\mathrm{shot}} = \frac{2h\nu_0}{P_0} \tag{86}$$

and

$$S_\varphi = \frac{h\nu_0}{2P_0} \tag{87}$$

4.3 Measurements of mixed spectra

In practice, a measured data may include simultaneously stationary white noise and "lines" (mains frequency multiples, resonances, etc.) and deterministic finite signal. If the data is calibrated in spectral density (for example $\mathrm{V}/\sqrt{\mathrm{Hz}}$), a doubling of the time acquisition will reduce by two the frequency resolution; the linear spectral density will be identical whereas line and signal amplitudes will raise by a factor $\sqrt{2}$, increasing signal to noise ratio. If the spectrum is calibrated in measurement units (for example V), then the line size will stay identical whereas the noise amplitude will be $\sqrt{2}$ smaller.

5 Digital synthesis of noise with arbitrary PSD

It may be necessary in certain contexts to model a time domain series with a given PSD.

5.1 Langevin's motor

In the case where $|H(f)|^2$ is a square modulus of a rational fraction of polynomials of variable if with real coefficients, then the noise $n(t)$ may be described as the convolution product

$$n(t) = h(t) \star g(t) \tag{88}$$

where $g(t)$ is a Gaussian white noise with $S_g = 1/\text{Hz}$ and $h(t)$ inverse Fourier transform of $H(f)$.

A digital implementation, with samples with period T_s, can be found with a recursion equation in the form of [28]

$$\begin{aligned} n[k] =& b_1 g[k] + b_2 g[k-1] + ... + b_N g[k-N+1] & (89)\\ &+ a_2 n[k-1] + ... + a_M n[k-M+1] & (90) \end{aligned}$$

which writes, with z transform, where $z = \exp(\text{i}2\pi f T_S)$,

$$n(z) = H(z) g(z) \tag{91}$$

with

$$H(z) = \frac{b_1 + b_2 z^{-1} + ... + b_N z^{-N+1}}{1 + a_2 z^{-1} + ... + a_M z^{-M+1}} \tag{92}$$

$H(z)$ can be deduced from $H(f)$ with, for example, a bilinear transformation, as in Python scipy.signal.bilinear(). The recursion equation for $n[k]$ is computed with scipy.signal.lfilter(). For a first-order filter there is a recursion relation simpler than the one with a bilinear transform, for a filter of amplitude 1, time constant τ, sampling time T_s:

$$n[k] = \text{e}^{-T_s/\tau} n[k-1] + \left(1 - \text{e}^{-T_s/\tau}\right) g[k]. \tag{93}$$

5.2 Arbitrary PSD

The aim is to generate a time series with a given $S_n(f)$, for example proportional to $1/f$, not feasible with a Langevin motor. This is also useful to test various PSD estimators.

The series will consist in $2N+2$ points sampled with period T_s. The frequency step in the PSD is $\Delta F = 1/((2N+2)T_s)$.

We use equation 6. The vector of $n(f)$ for positive frequencies is generated with a series of $2N$ random numbers with a normal Gaussian distribution. The quadratures are multiplied with $\sqrt{S_n(f)\Delta F/4}$. The two auxiliary degrees of freedom are the average and semi-alternate sum at Nyquist frequency; these values can be set to zero. The values for negative frequencies is set with complex conjugation. The final inverse Fourier transforms gives the series. A Python implementation is for example:

```
def PSD2TD (xPSD, fmin):
        #PSD2TD (PSD, fmin)
        # generate time-domain data
        # for gaussian noise with given PSD
        #
        # input:
        #     PSD : an array of PSDvalues, equally spaced in frequency,
        #               with interval fmin
        #           array has length N
        #     fmin: first frequency
        #           other frequencies to be n*fmin
        #            not zero!
        # output:
        #     t: time vector
        #     x:  data evenly spaced in time, with interval Ts
        # for input of size N, time data has size 2N+2

        v = xPSD*fmin/4 #variance for quadratures
        N = len(xPSD)
        vi = np.random.randn(N) # variance 1
        vq = np.random.randn(N)
        w = (vi + 1j*vq)*np.sqrt(v)

                # length of returned time sequence
        N_return = 2*(len(w)+1)

                # sampling time of returned time sequence
        Ts = 1/(N_return*fmin)

                # compute time vector
        x = np.fft.irfft(np.concatenate(([0], w, [0])),N_return)
                # add 0 amplitude at 0 frequency
                # add 0 amplitude at semi-alternate value
                # exact Nyquist frequency

        x = x*N_return
                # correct for inverse fft factor

        t  = np.linspace(0,Ts*(N_return-1),N_return)
                # prepare time vector for plots

        return t, x
```

Acknowledgements

The material in this paper is assembled from multiple interactions with colleagues, Ph.D. students, students in the lab as well as in the Virgo-LIGO-KAGRA gravitational wave detector instrument design and debugging community. The author has no conflict of interest to disclose.

Updates

Please send comments and suggested revisions to francois.bondu@univ-rennes.fr

References

[1] Harald Cramér. "A Century with Probability Theory: Some Personal Recollections." In: *The annals of Probability* 4.4 (1976), pp. 509–546.

[2] D.B. Percival and A.T. Walden. *Spectral Analysis for Physical Applications : Multitaper and Conventional Univariate Techniques*. Cambridge university press, 1993. ISBN: 978-0-521-43541-3.

[3] D.J. Thomson. "Spectrum Estimation and Harmonic Analysis." In: *Proceedings of the IEEE* 70.9 (Sept. 1982), pp. 1055–1096. ISSN: 0018-9219. DOI: 10.1109/PROC.1982.12433.

[4] Albert Einstein. "Méthode Pour La Détermination de Valeurs Statistiques d'observations Concernant Des Grandeurs Soumises à Des Fluctuations Régulières." In: *Compte rendu de la séance de la société suisse de physique* (28 février 1914), pp. 254–257.

[5] Norbert Wiener. "Generalized Harmonic Analysis." In: *Acta Mathematica* 55 (1930), pp. 112–258.

[6] A. Khintchine. "Korrelationstheorie der stationären stochastischen Prozesse." In: *Mathematische Annalen* 109.1 (Dec. 1934), pp. 604–615. ISSN: 0025-5831, 1432-1807. DOI: 10.1007/BF01449156.

[7] Peter D. Welch. "The Use of Fast Fourier Transform for the Estimation of Power Spectra: A Method Based on Time Averaging over Short, Modified Periodograms." In: *IEEE Transactions on Audio and Electroacoustics* 15.2 (June 1967), pp. 70–73. ISSN: 0018-9278. DOI: 10.1109/TAU.1967.1161901.

[8] Frederic J. Harris. "On the Use of Windows for Harmonic Analysis with the Discrete Fourier Transform." In: *Proceedings of the IEEE* 66.1 (Jan. 1978), pp. 51–63.

[9] Gerhard Heinzel, Albrecht Rüdiger, and Roland Schilling. *Spectrum and Spectral Density Estimation by the Discrete Fourier Transform (DFT), Including a Comprehensive List of Window Functions and Some New at-Top Windows*. 2002.

[10] D. Slepian and H. O. Pollak. "Prolate Spheroidal Wave Functions, Fourier Analysis and Uncertainty — I." In: *Bell System Technical Journal* 40.1 (Jan. 1961), pp. 43–63. ISSN: 1538-7305. DOI: 10.1002/j.1538-7305.1961.tb03976.x.

[11] H. J. Landau and H. O. Pollak. "Prolate Spheroidal Wave Functions, Fourier Analysis and Uncertainty — II." In: *Bell System Technical Journal* (1961).

[12] D. Slepian. "Prolate Spheroidal Wave Functions, Fourier Analysis and Uncertainty — V: The Discrete Case." In: *Bell System Technical Journal* 57.5 (1978).

[13] D. J. Thomson. "Jackknifing Multitaper Spectrum Estimates." In: *IEEE Signal Processing Magazine* 24.4 (July 2007), pp. 20–30. ISSN: 1053-5888. DOI: 10.1109/MSP.2007.4286561.

[14] Jeffrey Park, Craig R. Lindberg, and Frank L. Vernon. "Multitaper Spectral Analysis of High-Frequency Seismograms." In: *Journal of Geophysical Research: Solid Earth* 92.B12 (Nov. 1987), pp. 12675–12684. ISSN: 2156-2202. DOI: 10.1029/JB092iB12p12675.

[15] Germán A. Prieto. "The *Multitaper* Spectrum Analysis Package in Python." In: *Seismological Research Letters* 93.3 (May 2022), pp. 1922–1929. ISSN: 0895-0695, 1938-2057. DOI: 10.1785/0220210332.

[16] German A Prieto. *https://github.com/gaprieto/multitaper*. 2022.

[17] William H. Press et al. "Multitaper Methods and Slepian Functions." In: *Numerical Recipes*. 13.4.3. Cambridge University Press, 2007.

[18] L. Wang. "A Review of Prolate Spheroidal Wave Functions from the Perspective of Spectral Methods." In: *Journal of Mathematical Study* 50.2 (June 2017), pp. 101–143. ISSN: 1006-6837, 2617-8702. DOI: 10.4208/jms.v50n2.17.01.

[19] James Bremer. "On the Numerical Evaluation of the Prolate Spheroidal Wave Functions of Order Zero." In: *arXiv:2111.07509 [cs, math]* (Nov. 2021). arXiv: 2111.07509 [cs, math].

[20] "IEEE Standard Definitions of Physical Quantities for Fundamental Frequency and Time Metrology–Random Instabilities." In: *IEEE Std Std 1139-2008* (Feb. 2009), pp. 1–50. DOI: 10.1109/IEEESTD.2009.9464896.

[21] Phuong-Anh Huynh et al. "Status of GAP : An Electrostatic Accelerometer for Interplanetary Fundamental Physics." In: *65th International Astronautical Congress*. Toronto, Canada, 2014, IAC-14–A2.1.1.

[22] Diego Bersanetti et al. "Advanced Virgo: Status of the Detector, Latest Results and Future Prospects." In: *Universe* 7.9 (Sept. 2021), p. 322. ISSN: 2218-1997. DOI: 10.3390/universe7090322.

[23] *How to Measure Acurately Using the Agilent Combination Analysers*. Tech. rep. Agilent Note 4395/96-1. 1996.

[24] *Measuring with Modern Spectrum Analyzers*. Tech. rep. Rohde & Schwartz Educational Note 1MA201_09e. 2013.

[25] LIGO Scientific Collaboration and Virgo Collaboration et al. "Observation of Gravitational Waves from a Binary Black Hole Merger." In: *Physical Review Letters* 116.6 (Feb. 2016), p. 061102. DOI: 10.1103/PhysRevLett.116.061102.

[26] Frédéric de Coulon. *Théorie et Traitement Des Signaux*. Presses Polytechniques et Universitaires Romandes. Traité d'électricité VI. École Polytechnique Fédérale de Lausanne, 1996. ISBN: 2-88074-319-2.

[27] S. J. Orfanidis. *Electromagnetic Waves and Antennas*. 2004.

[28] Murat Kunt. *Traitement Numérique Des Signaux*. Vol. XX. Traité d'électricité. École Polytechnique Fédérale de Lausanne: Presses Polytechniques et Universitaires Romandes, 1996. ISBN: 2-88074-352-4.

Contents